

Magnetic susceptibility studies of the $(\text{Cr}_{98.4}\text{Al}_{1.6})_{100-x}\text{Mo}_x$ alloy system

B Muchono^{1,2}, C J Sheppard¹, A R E Prinsloo¹ and H L Alberts¹

¹ Physics Department, University of Johannesburg, P.O. Box 524, Auckland Park, Johannesburg 2006, South Africa

² Applied Physics Department, National University of Science and Technology, Box AC939, Ascot, Bulawayo, Zimbabwe

E-mail: alettap@uj.ac.za

Abstract. The magnetic susceptibility as a function of temperature, $\chi(T)$, on a spin-density-wave antiferromagnetic $(\text{Cr}_{98.4}\text{Al}_{1.6})_{100-x}\text{Mo}_x$ alloy system in the concentration range $0 \leq x \leq 8.8$ is reported in order to investigate the possibility of quantum critical behaviour in this alloy system. Néel temperatures, T_N , obtained from $\chi(T)$ measurements decrease with Mo concentration and sharply tend towards 0 K at a critical concentration $x_c \approx 4.5$. Antiferromagnetism is suppressed to below 4 K in alloys with $x \gtrsim 4.5$. Alloys in the concentration range $0 \leq x \leq 3.0$ depict an upturn in the $\chi(T)$ curves just above the Néel temperature. The upturn is attributed to local magnetic moments formed around the impurity atoms. The magnetic phase diagram of the alloy system points towards the existence of a quantum critical point at the critical concentration $x = x_c$. The suggestion of quantum critical behaviour in this alloy system from previous electrical resistivity(ρ), Seebeck coefficient (S) and specific heat (C_p) measurements is corroborated in this study.

1. Introduction

Studies of the physical properties of Cr and its alloys around the quantum critical point (QCP) have been a topic of interest in recent years [1-8]. The first experimental investigation of quantum critical behaviour in Cr alloys was done by Yeh *et al.* [8] on a $\text{Cr}_{100-y}\text{V}_y$ alloy system through chemical doping by V solute atoms. Tuning this alloy system through chemical doping across the QCP at the low temperature limit ($T \rightarrow 0$ K) induces an antiferromagnetic (AFM) to paramagnetic (P) phase transition on increasing y [8]. Quantum and not classical fluctuations at $T \approx 0$ K across a QCP cause a de-pairing effect of the electron-hole pairs resulting in an increase in the charge carrier density [3]. This has large effects on several physical properties such as the Hall number, $(qR_H)^{-1}$, and magnetic susceptibility, which both give an indication of the number of charge carriers at the Fermi surface (FS) [8]. Possible quantum critical behaviour was recently reported in the $(\text{Cr}_{98.4}\text{Al}_{1.6})_{100-x}\text{Mo}_x$ alloy system through $\rho(T)$, $S(T)$ and $C_p(T)$ measurements [1]. The Néel temperature for this alloy system decreases with x and disappears near a critical concentration $x_c \approx 4.5$ [1]. At the critical concentration the Sommerfeld specific heat coefficient as a function of x , $\gamma(x)$, depicts a peak similar to that observed in the archetypical quantum critical spin-density-wave (SDW) $\text{Cr}_{100-y}\text{V}_y$ alloy system [9].

Local magnetic moments were furthermore reported to exist in Cr doped with non-magnetic elements such as Al [10, 11] and V [12-16]. The $1/\chi$ versus T curves of these alloys follow a Curie-

Weiss (C-W) law just above T_N . The local magnetic moments in these alloys are formed above T_N , unlike those of Cr alloys doped with magnetic elements such as Fe and Mn, which are found to exist in both the P and AFM phases [15, 16].

Investigation of quantum critical behaviour in the $(\text{Cr}_{98.4}\text{Al}_{1.6})_{100-x}\text{Mo}_x$ alloy system is extended in this study through $\chi(T)$ measurements as complementary to the previous $\rho(T)$, $S(T)$ and $C_p(T)$ measurements [1]. The present study also investigates the possibility of having local magnetic moments in this alloy system as observed in the $\text{Cr}_{100-z}\text{Al}_z$ [10] alloy system.

2. Experimental

Polycrystalline ternary $(\text{Cr}_{98.4}\text{Al}_{1.6})_{100-x}\text{Mo}_x$ alloys in the range $0 \leq x \leq 8.8$ were prepared by repeated arc melting in purified argon atmosphere from 99.999 wt.% pure Cr, 99.999 wt.% pure Al and 99.99 wt.% pure Mo. The alloys were separately sealed into quartz ampoules filled with ultra-high purity argon and annealed at 1300 K for 3 days after which they were quenched into iced water. The composition of Cr, Al, and Mo in each alloy matrix was checked by electron microprobe analyses and the alloys were found to be of good homogeneity [1]. Spark erosion techniques were used to cut and plane the samples into disc shapes of approximately $2 \times 5 \text{ mm}^2$. The magnetic susceptibility measurements were done in the temperature range $4 \text{ K} \leq T \leq 300 \text{ K}$ using the Quantum Design Magnetic Property Measurement System (MPMS). The samples were initially zero field cooled to 4 K and then measurements were done in a constant applied magnetic field of 100 Oe while warming from 4 K to 300 K.

3. Results and discussion

Figure 1 shows representative examples of the $\chi(T)$ curves for the AFM $(\text{Cr}_{98.4}\text{Al}_{1.6})_{100-x}\text{Mo}_x$ system in the concentration range $0 \leq x \leq 4.3$. The alloys show clear anomalous $\chi(T)$ behaviour in the form of a sharp peak characterised by valley, a systematic upturn and a sudden downturn on cooling through T_N shown by arrows in the figure. The peak is weak and broad for an alloy with $x = 3.8$ (not shown) and becomes smeared out for the alloy with $x = 4.3$. The minimum χ -value of the valley observed above T_N for the alloys in the range $0 \leq x \leq 2.3$ decreases relative to the χ -value at T_N , with an increase in Mo content, but increases on further addition for alloys in the range $3.0 \leq x \leq 4.3$. The downturn observed in these alloys just below T_N is a typical behaviour of the SDW Cr and its alloys [17] and is attributed to a decrease in the density of states at the Fermi energy because of the appearance of a SDW energy gap when the samples are cooled through T_N [17]. On the other hand the downturn observed in the $\chi(T)$ curve just above T_N was also observed in the $\text{Cr}_{100-z}\text{Al}_z$ [10, 11] and $\text{Cr}_{100-y}\text{V}_y$ [12-16] alloys and was attributed to possible local magnetic moments formed around the Al and V impurity atoms, respectively. Just above T_N the curves of these alloys obey a C-W law given by [17]:

$$\chi(T) = \frac{C}{T - T_c}, \quad (1)$$

where T_c and C are the paramagnetic Curie temperature and C-W constant, respectively.

In order to confirm possible C-W behaviour in the present $(\text{Cr}_{98.4}\text{Al}_{1.6})_{100-x}\text{Mo}_x$ alloy system $1/\chi$ was plotted against T for alloys in the concentration range $0 \leq x \leq 3.0$ as shown in figure 2. The indicated straight lines represent fits of equation (1) through the data points. The lines give a positive gradient confirming the C-W behaviour in these alloys [16]. It can be concluded that in the present $(\text{Cr}_{98.4}\text{Al}_{1.6})_{100-x}\text{Mo}_x$ alloys local magnetic moments seem to be formed in the temperature range $T_N \leq T \leq 190 \text{ K}$ and $T_N \leq T \leq 170 \text{ K}$ for alloys with $x = 0, 0.7$ and 1.1 , respectively, and in the temperature range $T_N \leq T \leq 90 \text{ K}$ for the alloy with $x = 3.0$. Below T_N in figure 2, $1/\chi(T)$ abruptly increases as the C-W behaviour is superseded by antiferromagnetism. Thus, the origin of the upturn at $T > T_N$ for the present alloy system is probably ascribed to the C-W behaviour.

There is also a second upturn, more prominent in figure 1(d), present at low temperatures on the $\chi(T)$ curves of figure 1, presumably arising from upturn effects of a Curie tail [18], connected to oxide impurities [1]. The broken lines in figures 1(a) to (c) were drawn from the P phase and extend into the AFM phase to indicate the behaviour of the curves if they were to remain paramagnetic below T_N .

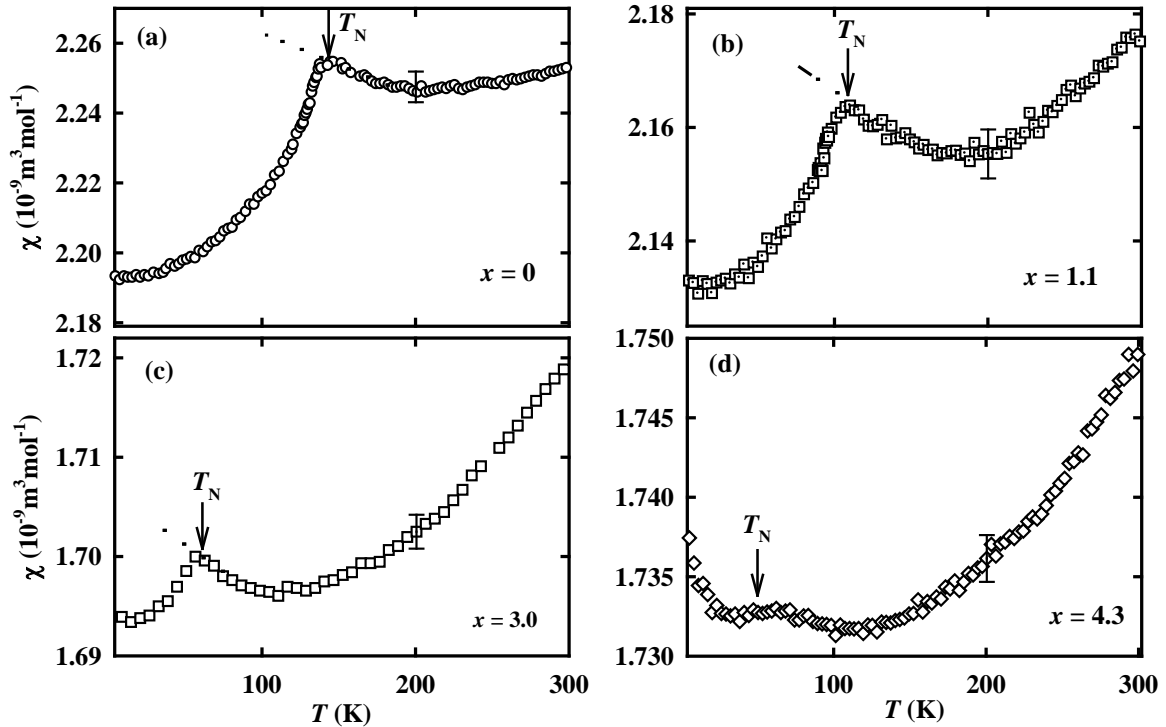


Figure 1. Magnetic susceptibility as a function of temperature, $\chi(T)$, for the $(\text{Cr}_{98.4}\text{Al}_{1.6})_{100-x}\text{Mo}_x$ alloys with (a) $x = 0$, (b) $x = 1.1$, (c) $x = 3.0$ and (d) $x = 4.3$. The broken lines in (a) to (c) are lines drawn from the P phase extending into the antiferromagnetic phase to indicate the behaviour of the alloys if they were to remain paramagnetic below T_N . The arrows in (a) to (c) indicate the T_N values obtained from the $\chi(T)$ curves while in (d) the arrow indicates T_N obtained from $\rho(T)$ measurements [1].

The values of T_N were obtained from the temperature where the measured $\chi(T)$ curves deviate from the broken lines. The broad peak anomaly observed on the alloy with $x = 4.3$ makes it difficult to precisely locate T_N . The arrow in figure 1(d) indicates T_N obtained from $\rho(T)$ measurements [1].

Figure 3 shows $\chi(T)$ measurements for the $(\text{Cr}_{98.4}\text{Al}_{1.6})_{100-x}\text{Mo}_x$ alloys in the concentration range $4.8 \leq x \leq 8.8$. These alloys did not show an anomalous $\chi(T)$ behaviour associated with SDW effects and were taken to be paramagnetic at all temperatures down to 4 K. $\rho(T)$ and $S(T)$ measurements of these alloys also showed these samples are P down to 2 K [1]. There is a peak observed in the susceptibility data for $x = 6.3$, however, the origin of this peak is unclear at present. It should be noted that $\rho(T)$ and $S(T)$ data for the $x = 6.3$ sample did not show any transitions associated with AFM behaviour at this temperature [1]. The upturn at low temperature observed for alloys with $x = 4.8, 6.3$ and 7.5 is also ascribed to oxide impurity effects, as described above.

Figure 4 shows the magnetic phase diagram of $(\text{Cr}_{98.4}\text{Al}_{1.6})_{100-x}\text{Mo}_x$ alloy system obtained from $\chi(T)$ curves of figures 1 and 3. T_N for alloys in the concentration range $0 \leq x \leq 3.8$ decreases with x . Antiferromagnetism disappears for alloys with $x \geq 4.8$. The alloy with $x = 4.3$ shows a slightly higher value of T_N compared to the alloy with $x = 3.8$. The higher value of T_N for this alloy is probably because of an overlap of the Curie tail discussed above and the onset of antiferromagnetism, making it difficult to locate T_N for $x = 4.3$. A similar $T_N(x)$ graph was observed for this alloy system through $\rho(T)$ measurements [1]. The solid line shown in figure 4 is a power law fit through the data points. The fit is of the form:

$$T_N = a(x_c - x)^b, \quad (2)$$

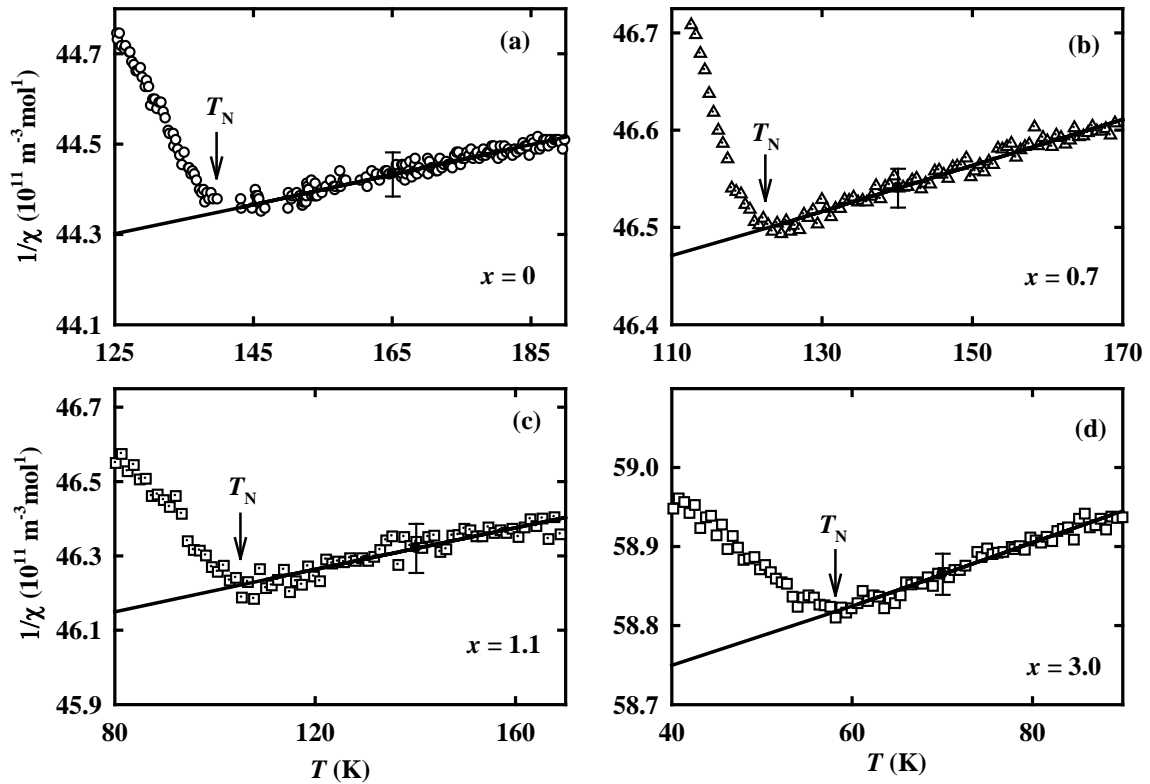


Figure 2. $1/\chi$ as a function of temperature for the $(\text{Cr}_{98.4}\text{Al}_{1.6})_{100-x}\text{Mo}_x$ alloys with (a) $x = 0$, (b) $x = 0.7$, (c) $x = 1.1$ and (d) $x = 3.0$. The solid lines are guides to the eye through the data points.

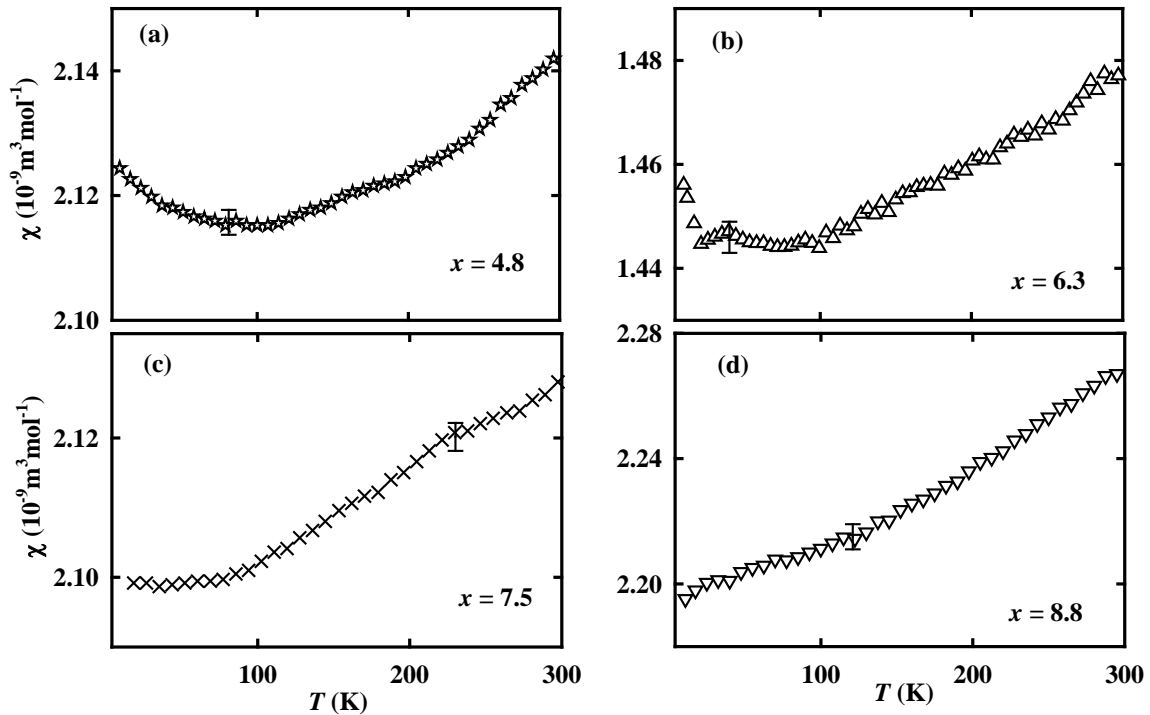


Figure 3. Magnetic susceptibility as a function of temperature, $\chi(T)$, for the $(\text{Cr}_{98.4}\text{Al}_{1.6})_{100-x}\text{Mo}_x$ alloys with (a) $x = 4.8$, (b) $x = 6.3$, (c) $x = 7.5$ and (d) $x = 8.8$.

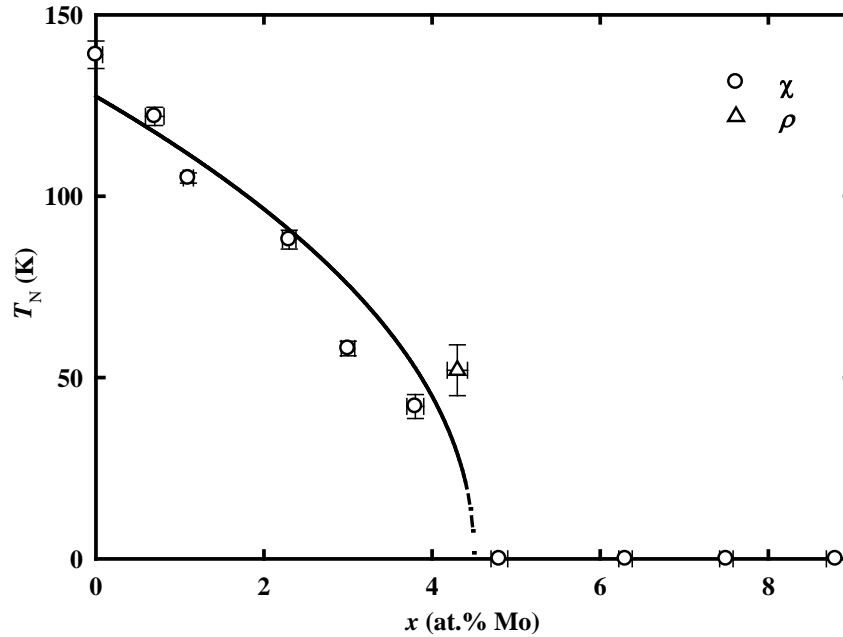


Figure 4. The Néel transition temperature, T_N , as a function of Mo concentration for the $(\text{Cr}_{98.4}\text{Al}_{1.6})_{100-x}\text{Mo}_x$ alloy system obtained from (○) the $\chi(T)$ curves of figures 1 and 3, and (△) $\rho(T)$ measurements. The solid line is a power law fit through the data points. The error in the data points is represented by the error bars.

where $a = 62 \pm 10$ K is a fitting parameter, $b = 0.5 \pm 0.1$ is a critical exponent and $x_c = 4.50 \pm 0.01$ is a critical concentration where antiferromagnetism disappears. The addition of Mo to the mother alloy $\text{Cr}_{98.4}\text{Al}_{1.6}$ decreases the strength of antiferromagnetism through electron hole pair breaking effects due to electron scattering and a delocalization of the 3-d bands in Cr on introducing the 4-d bands of Mo [17].

The critical exponent b in equation (1) is an important parameter in magnetic systems that approach quantum criticality at low temperatures when an order parameter such as impurity concentration, pressure or magnetic field is varied [19]. The mean field theory for such systems predicts the critical exponent $b \approx 0.5$ [19]. Clearly the value of the critical exponent obtained from the present study is in line with mean field theory. It also compares fairly well with those obtained from electrical resistivity measurements in $T_N \propto (x_c - x)^{0.4 \pm 0.1}$ and $\Delta\rho_0/\rho_0 \propto (x_c - x)^{0.5 \pm 0.1}$ [1] of the same alloy system. These values are also in line with those obtained by Jaramillo *et al.* [3], Lee *et al.* [4] and Reddy *et al.* [5] in the electrical resistivity measurements of pressure tuned Cr and $\text{Cr}_{96.8}\text{V}_{3.2}$ single crystals, and chemical doped $(\text{Cr}_{86}\text{Ru}_{14})_{100-u}\text{V}_u$ polycrystalline alloys, respectively.

4. Conclusion

Magnetic susceptibility studies on the $(\text{Cr}_{98.4}\text{Al}_{1.6})_{100-x}\text{Mo}_x$ alloy system showed that antiferromagnetism in this system is completely suppressed to below 4 K at the critical concentration $x_c \approx 4.5$. Previous $\rho(T)$ results for this alloy system also showed a suppression of antiferromagnetism to below 2 K at the same concentration. At x_c the $\gamma(x)$ for the same alloy system depicts a peak similar to that observed in the archetypical quantum critical spin-density-wave $\text{Cr}_{100-y}\text{V}_y$ alloy system. The value of the critical exponent b of equation (1), obtained from figure 4, is in line with that expected from the mean field theory. Alloys in the concentration range $0 \leq x \leq 3.0$ depict a valley just above T_N indicating the presence of local magnetic moments in these alloys similar to those reported in the $\text{Cr}_{100-z}\text{Al}_z$ and $\text{Cr}_{100-y}\text{V}_y$ alloy systems. The present results and the previous findings point towards the existence of a possible quantum critical point around $x \approx 4.5$.

Acknowledgements

Financial support from the South African National Research Foundation (Grant numbers 80928 and 80626) and the Faculty of Science from the University of Johannesburg are acknowledged.

References

- [1] Muchono B, Sheppard C J, Prinsloo A R E, Alberts H L and Strydom A M 2014 *J. Magn. Magn. Mater.* **354** 222
- [2] Jacobs B S, Prinsloo A R E, Sheppard C J and Strydom A M 2013 *J. Appl. Phys.* **113** 17E126
- [3] Jaramillo R, Feng Y, Wang J and Rosenbaum T F 2010 *PNAS.* **107** 13631
- [4] Lee M, Hussman A, Rosenbaum T F and Aeppli G 2004 *Phys. Rev. Lett.* **92** 187201
- [5] Reddy L, Alberts H L, Strydom A M, Prinsloo A R E and Venter A M 2010 *J. Appl. Phys.* **103** 07C903
- [6] Sheppard C J, Prinsloo A R E, Fernando P R, Venter A M, Strydom A M and Peterson A M 2013 *J. Appl. Phys.* **113** 17E146
- [7] Varella A L S and de Oliveira A J A 2010 *J. Phys.: Conf. Ser.* **200** 012025
- [8] Yeh A, Soh Y A, Brooke J, Aeppli G, Rosenbaum T F and Hayden S M 2002 *Nature* **419** 459
- [9] Takeuchi J, Sasakura H and Masuda Y 1980 *J. Phys. Soc. Jpn.* **49** 508
- [10] Sheppard C J, Prinsloo A R E, Alberts H L, Muchono B and Strydom A M 2014 *J. Alloys and Compounds* **595** 164
- [11] Sousa J B, Amado M M, Pinto R P, Pinheiro M F, Braga M E, Moreira J M, Hedman L E, Åström H U, Khlaif L, Walker P, Garton G and Hukin D 1980 *J. Phys. F: Metal Phys.* **10** 2535
- [12] Fawcett E 1992 *J. Phys.: Condens. Matter* **4** 923
- [13] Hill P, Ali N, de Oliveira A J A, Ortiz W A, de Camargo P C and Fawcett E 1994 *J. Phys. Condens. Matter* **6** 1761
- [14] de Oliveira A J A, de Lima O F, de Camargo P C, Ortiz W A and Fawcett E 1996 *J. Phys.: Condens. Matter* **8** L403
- [15] de Oliveira A J A, Ortiz W A, de Camargo P C and Galkin V Y 1996 *J. Magn. Magn. Mater.* **152** 86
- [16] de Oliveira A J A, Ortiz W A, de Lima O F and de Camargo P C 1997 *J. Appl. Phys.* **81** 4209
- [17] Fawcett E, Alberts H L, Galkin V Y, Noakes D R and Yakhmi J V 1994 *Rev. Mod. Phys.* **66** 25
- [18] Wagner M J, Dye J L, Pérez-Condero E, Bulgas R and Echevoyen L 1995 *J. Am. Chem. Soc.* **117** 1318
- [19] Hertz J A 1976 *Phys. Rev. B* **14** 1165